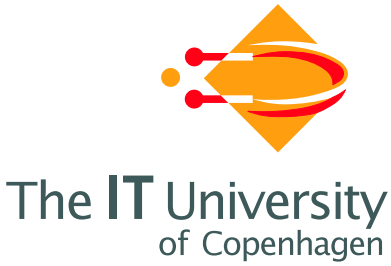

Simplifying Structures by Selectively Specifying Suited Scale Space Saddles

Arjan Kuijper

IT University Technical Report Series **TR-2004-53**

ISSN 1600–6100 **December 2004**

ISSN 1600–6100

ISBN 87-7949-075-1

Copies may be obtained by contacting:

IT University of Copenhagen
Rued Langgaards Vej 7
DK-2300 Copenhagen S
Denmark

Telephone: **+45 72 18 50 00**
Telefax: **+45 72 18 50 01**
Web `www.itu.dk`

Contents

Abstract

Blurring an image with a Gaussian of width σ and considering σ as an extra dimension, extends the image to an Gaussian scale space ($\mathcal{GSS}$) image. In this $\mathcal{GSS}$-image the iso-intensity manifolds behave in an nicely predetermined manner. As a result of that, the $\mathcal{GSS}$-image directly generates a hierarchy in the form of a binary ordered rooted tree, that can be used for segmentation, indexing, recognition and retrieval. Understanding the geometry of the manifolds allows fast implementational methods to derive the hierarchy. Scale space saddles form the pivot for this hierarchy. However, not all scale space saddles are relevant. The key to solve this ambiguity is the investigation of both the scale space saddles and the iso-intensity manifolds through them. In this paper the different situations that one can encounter in this investigation are described, the relevant scale space saddles are pointed out, examples are given and the difference between selecting the relevant and the non-relevant ("void") scale space saddles is shown. Next, the relevant geometric properties of $\mathcal{GSS}$ images is discussed, as well as their implications for algorithms used for the tree extraction. It appears that one doesn't need to search through the whole $\mathcal{GSS}$ image to find regions related to each relevant scale space saddle. Examples show the applicability and increased speed of the proposed method compared to traditional ones.

1 Introduction

When images are considered, they are always considered at some scale. Often the focus is on single pixels - the so-called inner scale - in case of enhancement. However, at the same time also intermediate structures - scales - are relevant, since it is important to know if either noise or 'relevant data' is enhanced. So in image analysis most operators intrinsically have some size, or scale. Inevitably, if one is not aware of this fact, the wrong scale can be used. One way to avoid this risk is by taking into account all possible, reasonable, scales.

Since there exists a huge pile of possible multi-scale methods, it makes sense to restrict to those that have a firm mathematical and reasonable axiomatic basis. In the first group so-called test-functions are found, that transfer the discrete data into the continuous domain [38]. In the latter group those axioms are prefered that state that 'we know nothing of the image' [16]. The basic operator for just observing an image - an array of discrete numbers - under some almost trivial assumptions like linearity, isotropy, no preferred direction or scale, and separability of the kernel then becomes a *Gaussian filter*, as argued by Florack et al. [12]. This well-known filter appears to be at the intersection of both approaches.

1.1 Scale Space

The gist of a so-called *Gaussian scale space* originated from Koenderink [22] and Witkin [41] with as starting point the non-enhancement of local extrema of the signal [41] or image [22] as the scale increases. However, some twenty years earlier scale space was already introduced in Japanese literature by Ijimia [18, 19].

When an image is blurred with a Gaussian filter, the scale (the width, or variance of the filter) needs to be chosen. The Gaussian scale space paradigm [10, 19] states in contrast that *no* scale should be chosen in advance. The $(n)-$ dimensional image is thus extended to an $(n+1)-$dimensional Gaussian scale space ($\mathcal{GSS}$) image. Although several books on scale space, e.g. [10, 15, 34, 39, 40], and much literature have appeared and biannually scale space conferences [17, 21, 36] are held, the exploration of the so-called *deep structure* of Gaussian scale space – i.e. the image at all scales simultaneously – is still premature. Mostly scale space is used as a tool, while the tool itself is not investigated.

Some results on the deep structure - the complete structure - of $\mathcal{GSS}$ images are reported, albeit that most results describe local situations, like neighbourhoods of point-events like so-called catastrophe points [3] or saddle points [13, 23, 26].

1.2 Deep structure

Recently, novel results [26] were reported in the use of $\mathcal{GSS}$ images. In section 2, I will summarise the main results of this work leading to a unique uncommitted topological segmentation of the image. This is based on the hierarchical structure implicitly present in the scale space image and the movement of the critical points under blurring (increasing scale). Furthermore, a binary ordered rooted tree can be extracted that represents the hierarchy [29]. Of particular interest is the combination of *iso-intensity manifolds* and *saddle points*, both in the

scale space image. They were mentioned by Koenderink [22] and Griffin and Colchester [13]. The extraction of iso-manifolds in linear scale space for feature tracking has been reported by Fidrich [7, 8, 9]. She used intersections of two manifolds to determine curves representing differential invariants. Eberly discussed the geometrical properties of general scale spaces and appropriate metrics for them [6]. One result is that using a space with an Euclidean metric leads to the linear Gaussian scale space.

It appears that the iso-intensity manifolds through the scale space saddles provide necessary and sufficient information for the hierarchy and segmentation [24, 29, 26, 30, 31, 28, 27, 25]. A drawback of the extraction procedure as described in these papers, is their need for $(n+1)-$D region extraction. Since $\mathcal{GSS}$ images can be complicated, the procedure is computationally expensive. Meanwhile, however, these methods are in the state of evaluating their relevance with respect to image indexing and retrieval, as presented in [20].

1.3 New results

In this paper I elaborate on previous work [24, 26, 30, 27, 28, 31, 25] in which results on deep structure were presented. Here I discuss the *global geometrical structure* of $\mathcal{GSS}$ images, bridging the local events and the hierarchical tree structure and yielding a faster method to derive the latter based on the former, using the geometry of iso-manifolds in the $\mathcal{GSS}$ image. Before this stage, described in Section 4, can be reached, the issue of so-called *void* scale space saddles [24, 28, 25] with their corresponding manifolds needs to be dealt with. In section 3 I will present a classification of the iso-intensity manifolds as they can be found in the scale space image. It will be explained why "void" scale space saddles are *not* of interest for the hierarchy and segmentation.

Section 6 shows some applications and provides "visual" insight of the theory presented. Test images with void saddles and are presented and the correct hierarchy is derived. Next, numerical evidence is given for the increased speed of the algorithm.

Conclusions will be drawn and a discussion given in section 7.

2 Background: The Deep Structure of Gaussian Scale Space Images

In view of the ample literature on Gaussian scale space, only a brief introduction is given. The interested reader is referred to the literature mentioned in the introduction and references therein. Note that there are also non-linear scale spaces [15] and that besides a Gaussian scale space also other linear scale spaces exist [5]. In the remainder of this paper "scale space" is used as shorthand notation for "Gaussian scale space". Furthermore, a brief review of the deep structure of Gaussian scale space and the hierarchy in the $\mathcal{GSS}$ image is given.

2.1 Gaussian scale space

Let $L(\mathbf{x})$ be an image with $\mathbf{x}$ an n-dimensional spatial variable (point) and L the intensity measured at the point. In order to transfer the discrete image to the continuous domain, so-called test functions [38] are needed. Among those functions, the one is choosen that satisfies the constraints that it has no preferred orientation, size, location, and no memory. Finally, the function needs to be separable for computational purposes [16]. As a result, one ends up with the Gaussian filter [19, 34, 12]. Consequently, the *Gaussian scale space image* $L(\mathbf{x};t)$ is defined as the convolution of L with a Gaussian:

$$L(\mathbf{x};t) = \int_{R^n} \frac{1}{\sqrt{4\pi t}^n} e^{-\frac{|\mathbf{x}-\mathbf{y}|^2}{4t}} L(\mathbf{y})\, d\,\mathbf{y}$$

As one can verify, the Gaussian scale space image satisfies the diffusion equation: $\partial_t L(\mathbf{x};t) = \Delta L(\mathbf{x};t)$ and $\lim_{t\downarrow 0} L(\mathbf{x};t) = L(\mathbf{x})$. This is the result of an other axiom: causality, as suggested by Koenderink [22]. It boils down from the assumption that moving upwards in the $\mathcal{GSS}$ image no spurious details are created, and it thus implies that no new level lines are created. Generally, when blurring, structure disappears due to the pair-wise annihilation of a pair of critical points. It is, however, possible that locally an extremum and a saddle are pair-wise created [3].

These *critical points* of an image are those points with zero gradient: $\nabla_{\mathbf{x}} L(\mathbf{x}) = 0$. Their type is determined by the *Hessian matrix*, containing all mixed second order derivatives: $H(\mathbf{x}) = \nabla^T \nabla L(\mathbf{x})$. If all eigenvalues have

the same sign the point is an *extremum*, a *minimum* if all are positive and a *maximum* if all are negative. If the eigenvalues are both positive and negative, the point is a *saddle point*. If an eigenvalue is zero (and consequently $\det H = 0$), the point is degenerate and called *catastrophe point* [37] . For images this is non-generic, since it demands an extra requirement.

The concept of pairwise annihilation and creation of critical points automatically leads to the definition of *critical curves*: one-dimensional strings through the $\mathcal{GSS}$ image that satisfy $\nabla_x L(\mathbf{x}; t_i) = 0$ for each fixed t_i. Note that this is just a formal definition linking critical points over scale. The linking respects the type of critical point (maximum, saddle, minimum), and, as Damon showed [3], at so-called catastrophe points a saddle part and a extremum part meet. These points are the local extrema of the critical curve with respect to scale in the $\mathcal{GSS}$ image.

Therefore, critical curve generally consists of (spatial) extrema and saddle points as well as their connection points, the catastrophe points. At these points *generically* exactly one extremum and one saddle point are annihilated or created at increasing scale. For a thorough treatment of the non-trivial transfer of catastrophe theory [37] into scale space, see e.g. Damon [3, 4]. It roughly boils down to the fact that scale can be regarded as an extra parameter enabling the most simple catastrophe demanding only one parameter. So generically, critical curves don't intersect. The part of the critical curve containing extrema is called *extremum branch*, the one containing saddle *saddle branch*.

Under some conditions of the initial image like non-negativeness of the intensity and presence of a Jordan curve around all extrema [35], the image at some large scale contains only one extremum. As a consequence, all but one critical curves exist on a finite interval of scales. Most of them start and end in the initial image, even with "wiggles" when the curve increases, decreases and increases again due to the presence of a creation event [24, 27]. It should be noted that also closed loops can occur [24, 27].

2.2 Critical points in scale space

At *Scale space critical points* $\nabla_{\mathbf{x}} L(\mathbf{x}; t) = 0$ and $\partial_t L(\mathbf{x}; t) = 0$. The first requirement implies that scale space critical points are located on a critical curve. The second requirement equals $\Delta L(\mathbf{x}; t) = 0$ due to the diffusion equation. Consequently, it implies a zero trace of the (spatial) Hessian matrix, and thus both positive and negative eigenvalues, and scale space critical points *must* be scale space saddles [13, 23, 26, 31]. Note that for signals ($n = 1$) catastrophe points coincide with scale space saddles. For images of dimension larger than one this is non-generic.

From the definition of a scale space saddle it follows directly that at a critical curve the intensity has a local extremum at the scale space saddle: it will change from increasing ($\partial_t L(\mathbf{x}; t) > 0$) to decreasing ($\partial_t L(\mathbf{x}; t) < 0$) or vice versa. Consequently, scale space critical points can be found easily when the critical curve and its intensities are known. It thus makes sense to visualise the intensity of the critical curve as a function of scale. The extremum branches are monotonically decreasing (maximum) or increasing (minimum). Saddle curves wiggle if scale space saddles are present. At catastrophe points two curves come together with the same non-zero sign of $\partial_t L$ [13]. This is clear from the fact that when parameterising the critical curve in this whole space, the catastrophe point is a regular point [11].

2.3 Iso-intensity manifolds

As an extension of isophotes, *Iso-intensity manifolds* are manifolds with the same intensity throughout the $\mathcal{GSS}$ image. They encapsulate extrema and vanish at some scale. This is due to the property of "non-enhancement of local extrema", "maximum principle", or "non-creation of new level lines" [22, 34]. Note that this does not forbid creations of critical points. Consequently, iso-intensity manifolds in $(\mathbf{x}; t)$-space form closed "realms" [22]. They can be visualised as a mountain landscape [28] (a surface in a 3D scale space image, etc.), in which one or multiple tops are present. The number of tops depends on the number of spatial extrema on the manifold. This is visualized in Figure 1, where four different iso-intensity manifolds are shown, together with the critical curves. Each top of a manifold intersects an different extremum branch.

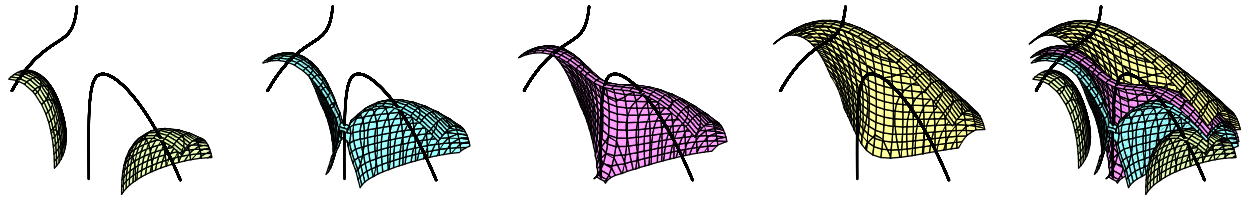

Figure 1: Iso-intensity manifolds and critical curves in scale space. From left to right the intensity increases. a) Two manifolds with one top. Each one intersects an extremum branch. b) They touch at the scale space saddle. c) One iso-intensity manifold remains with two tops, at each extremum branch one. d) The extremum manifold intersects only the left extremum branch. e) The nesting of the manifolds.

2.4 Scale space hierarchy

As Figure 1 may indicate, the nesting of the iso-intensity manifolds impose a hierarchical structure on the original image. Starting with the intensity of one extremum at the initial image, one finds a nesting of iso-intensity manifolds around this extremum (cf. the nesting of isophotes around an extremum in 2D).

At some intensity the manifold touches another manifold emerging from another extremum, cf. Figure 1b. This occurs at a scale space saddle, corresponds via the saddle branch and its critical curve to one of the extrema. So unique segments in scale space can be assigned to an extremum and the nesting of them results in the topological hierarchy tree, with scale space segments as branches and information of the scale space saddle and the catastrophe point as node (cf. Figure 1, where the right segment is related to the annihilating extremum). It enables an topological segmentation, since to each extremum a region is assigned [24, 26, 30].

Each critical curve can be related to a manifold, vice versa, and each annihilating extremum can be related to a scale space saddle. So the saddle relates two different critical curves, while both curves have a different maximal scale location (the annihilation point). The first disappearing curve causes its related manifold to be called *critical*.

In [26] a difference in the hierarchy based on the scale location of the disappearance of a critical curve related to the critical manifold is advocated, whereas in [29] the focus is changed to the location of the scale space saddle in the $\mathcal{GSS}$ image. The manifold that was nameless is called *dual* in that paper. An example is given in Figure 2. The left image shows two manifolds joining at the scale space saddle. The critical curve through it also intersects the right manifold. At the top of the curve an annihilation takes place involving the saddle part (left, through the scale space saddle) and an extremum part (right, intersecting the manifold at its top). Therefore, the right manifolds is called *critical*. Consequently, the left manifold is called *dual*. Note that this manifold is also intersected at the top by an (other) critical curve. The right image shows the corresponding tree structure. The scale space saddle SSS is a node with two children: the critical curve determined by critical manifold, edge C and the critical curve determined by the dual manifold, edge D. The edge to its parent P is formed by the critical curve determined by dual manifold. The parent is either the root, or another scale space saddle. In the latter case is the edge either labeled C or D.

In [26] the authors reported the existence of multiple scale space saddles on a saddle branch. This obviously results in multiple iso-intensity manifolds and extra nodes in the hierarchy tree. Questions rise in how far this is redundant or essential information. It also may influence the positions of the nodes in the hierarchy tree. In the following section I will answer these questions by classifying the manifolds that may be present. The key to solve this potential problem is given by the concept of *void scale space saddle*. This subset of scale space saddles is defined as those scale space saddles that do *not* connect two distinct iso-intensity manifolds.

3 Classification of manifolds

In this section the different types of manifolds in Gaussian scale space are given, as far as they are relevant for the hierarchy as described in the previous section. All manifolds in scale space contain either one or zero scale

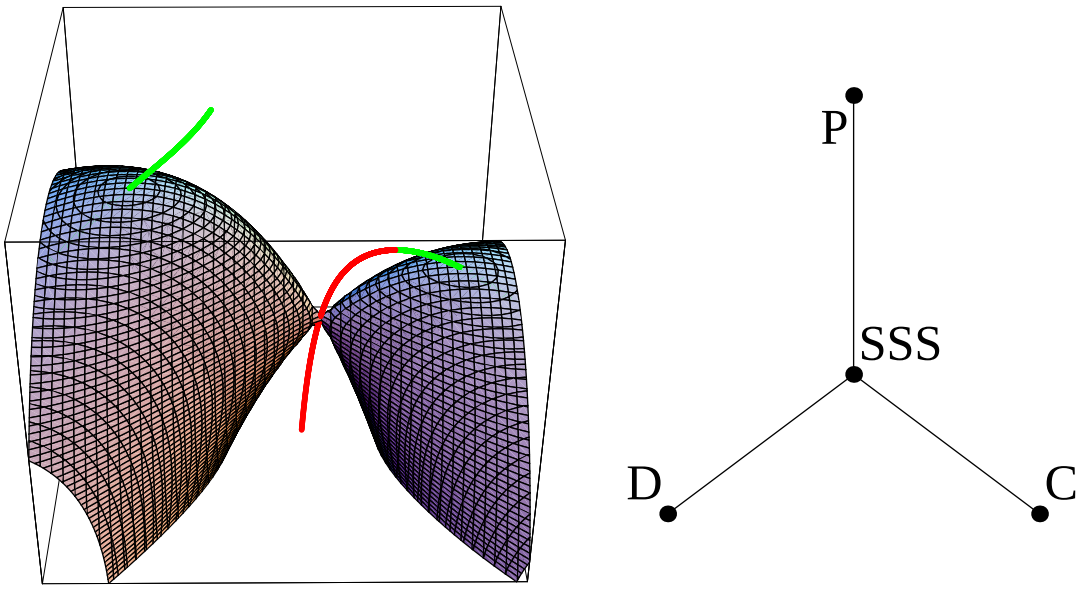

Figure 2: Left: A critical and a dual manifold joined at a scale space saddle. Right: Building block of the tree structure.

space saddles - by genericity, just as an isophote contains either one or zero spatial saddles. However, as will be clear in the remainder of this section, not all scale space saddles lie on iso-intensity manifolds that give rise to distinct segments in scale space. The segments are related to extrema, which are in turn related to extrema branches and consequently saddle branches. Therefore a classification is give based on the number of scale space saddles that a saddle branch contains.

In this classification I will only address critical curves containing a saddle branch that annihilates with a maximum. The saddle - minimum variant follows analogously. Since special interest lies in the behaviour of the iso-intensity manifolds through scale space saddles in relation with the hierarchical structure and induced topological segmentation, the combination annihilation - scale space saddle is taken. In this context creations are not relevant, since they are only protuberances of the critical curve [24, 27]. In the examples shown one can consider the first scale taken as either the initial scale or the creation scale. This makes no difference for understanding.

In the examples sets of two connected plots are given. The first plot shows the intensities of the saddle and maximum branch as a function of increasing scale. Consequently, the intensity of the maximum decreases monotonically: all its eigenvalues are negative and so their sum, equalling the trace of the Hessian and the scale derivative. The saddle branch is allowed to have multiple local extrema: the scale space saddles. The second plot visualises the iso-intensity manifolds in the 2D $(x;t)$-space, reducing them thus to isophotes. The remaining dimensions can be visualised by imagining this as a cross-section through a mountain landscape containing bridges at scale space saddles, cf. Figure 1.

Special attention must be paid to non-generic events. At a catastrophe points, $\det H = 0$, so one of the eigenvalues λ_i equals zero. The case that more eigenvalues are zero is non-generic. The same holds for a combination of them being zero. So generically, $\mathrm{tr}\, H \neq 0$ at a catastrophe point. For two dimensional images this implies that at a catastrophe point one eigenvalue is non-zero. In higher dimensional images, for example 3D, not only the case $\lambda_1 = \lambda_2 = \lambda_3 = 0$, but also cases like $\lambda_1 = -\lambda_3$ and $\lambda_2 = 0$ at a catastrophe point are *not* generic in 3D.

However, dealing with discrete images and finite precision, one may encounter non-genericities [28]. In this case the catastrophe point and a scale space saddle cannot be distinguished. In the following classification this can be visualised by coinciding the catastrophe point with the last scale space saddle before annihilation.

3.1 Zero scale space saddles

If the saddle branch does not contain any scale space saddles from the initial scale until the annihilation, the intensities of both the saddle and the maximum are decreasing, see Figure 3a. The largest value on the saddle branch is thus the value of the spatial saddle in the initial image (intensity 2). At this point two distinct manifolds intersect as shown in Figure 3b. At intensity 1, the one of the annihilation, there is only one manifold.

Example

Let $L(x, y; t) = \frac{1}{6}x^3 + xt - 3y^2 - 6t$ **for** $t \geq -10$**. Then the critical curve follows from** $\frac{1}{2}x^2 + t = 0$ **and** $-6y = 0$ **and is given by** $(x, y; t) = (\pm\sqrt{-2t}, 0; t)$ **for** $-10 \leq t \leq 0$**. The intensity of the critical curve is** $L_{\pm}(x(t), 0; t) = -6t \pm \frac{2}{3}t\sqrt{-2t}$**, for** $0 \geq t \geq -10$**. The determinant of the Hessian reads** $-6x$**, so the origin is the catastrophe point. For a potential scale space saddle** $\partial_t L = 0$**, yielding** $x - 6 = 0$**, i.e.** $t = -18$**, which is outside the scale domain. The intensities of the branches are both decreasing:** $\partial_t L_{\pm}(x(t), 0; t) = -6 \pm \sqrt{-2t}$**, which is negative in the scale domain.**

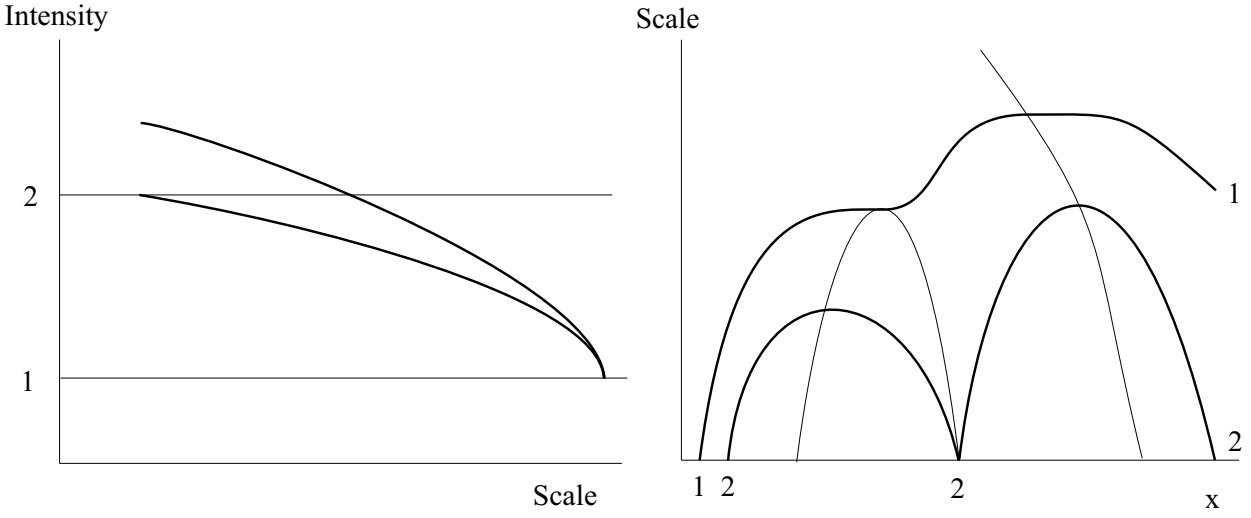

Figure 3: a: Intensities of the maximum (top) and saddle branch. No scale space saddle are present. b: Critical curves (thin) and Iso-intensity manifolds (thick) in the plane of the dominant spatial variable and scale. Intensity 1 at the catastrophe forms a manifold through the catastrophe point. Intensity 2 through the saddle point at the initial image separates two distinct manifolds.

3.2 One scale space saddle

If the saddle branch contains one scale space saddle, its intensity at it is larger than that at the catastrophe, see Figure 4a. The intensity of the saddle increases – passing intensity 1 – until it reaches the scale space saddle (intensity 2), and then decreases until its annihilation point (intensity 1).

The values on the saddle branch attained between the scale space saddle and the catastrophe point are also attained at some smaller scale. This is visible in Figure 4 where for intensities between 1 **and** 2**, the manifold has three intersections with the critical curve: two with the saddle branch and one with the maximum.**

Example

Take $L(x, y; t) = x^3 + 6xt - y^2 - 2t$**. The critical curve follows the path** $(x, y; t) = (\pm\sqrt{-2t}, 0; t)$ **for** $t \leq 0$**. Since the determinant of the Hessian is** $-12x$ **and its trace** $6x - 2$**, the maximum and the saddle annihilate at the origin, while the saddle branch (positive** x **values) contains a scale space saddle at** $(x, y; t) = (1/3, 0; -1/18)$**. The intensities on the critical curve are given by** $L_+(x(t), 0; t) = 4t\sqrt{-2t} - 2t$ **and** $L_-(x(t), 0; t) = -4t\sqrt{-2t} - 2t$**.**

One can verify that L_+ is decreasing strict monotonically, as it corresponds to the maximum. The saddle branch, L_-, contains a local maximum at $t = -1/18$.

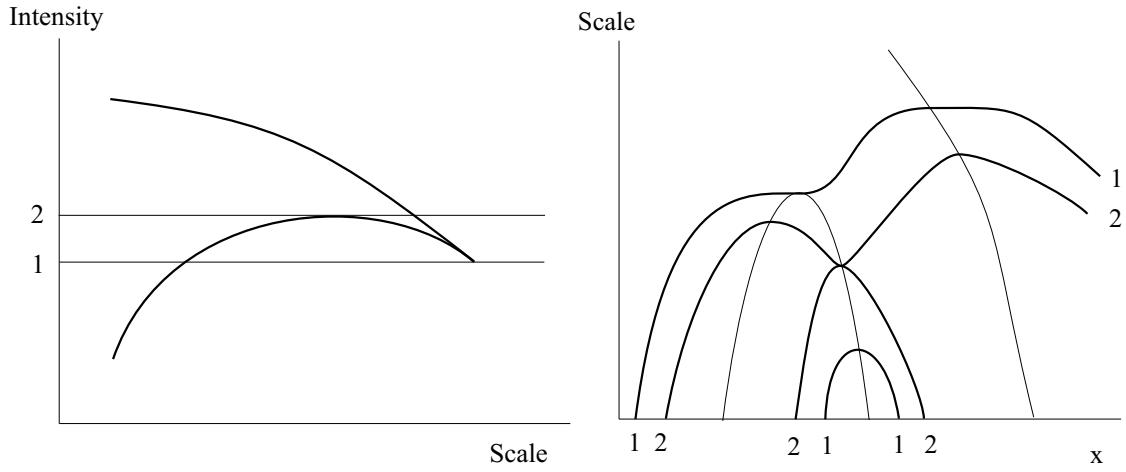

Figure 4: a: Intensities of the maximum (top) and saddle branch. b: Critical curves (thin) and Iso-intensity manifolds (thick) in the plane of the dominant spatial variable and scale. At the scale space saddle two distinct manifolds intersect.

3.3 Two scale space saddles

Recalling Figure 4, a saddle branch with an extra scale space saddle can occur in two cases: The intensity of the second scale space saddle is either larger than the catastrophe point (case A), or smaller (case B).

3.3.1 Case A

The first case is visualised in Figure 5. Since the number of scale space saddles is even, the intensity of the saddle in the initial image (intensity 4) is taken to derive two distinct manifolds. Now the scale space saddle with intensity 3 intersects the saddle branch also at a smaller scale: it is the part of a manifold that intersects itself. The same analogy holds for the scale space saddle with intensity 2. It is part of the manifold through both branches that is wrapped around the manifold with intensity 3. Consequently, both scale space saddles are void.

3.3.2 Case B

In the second case, the intensity of the catastrophe point lies between those of the scale space saddles, see figure 5. Again the intensity of the saddle in the initial image (intensity 4) yields two distinct manifolds and the scale space saddles do not connect distinct manifolds. Only the one with intensity 3 is related to a manifold through the extremum branch. The other one is not related to the critical curve. Again, both scale space saddles are void.

3.4 More scale space saddles

This classification can be infinitely extended as one can imagine. However, inserting more scale space saddles basically implies inserting more local extrema on a saddle branch and thus inserting more self-intersecting locations of an iso-intensity manifold and thus inserting void scale space saddles. This holds unless, of course, when the intensity of a newly inserted scale space saddle is the local maximum on the saddle branch – still regarding maximum-saddle annihilations. In case of minimum-saddle annihilations "highest" becomes "lowest", and so on. The classification thus follows the following rules:

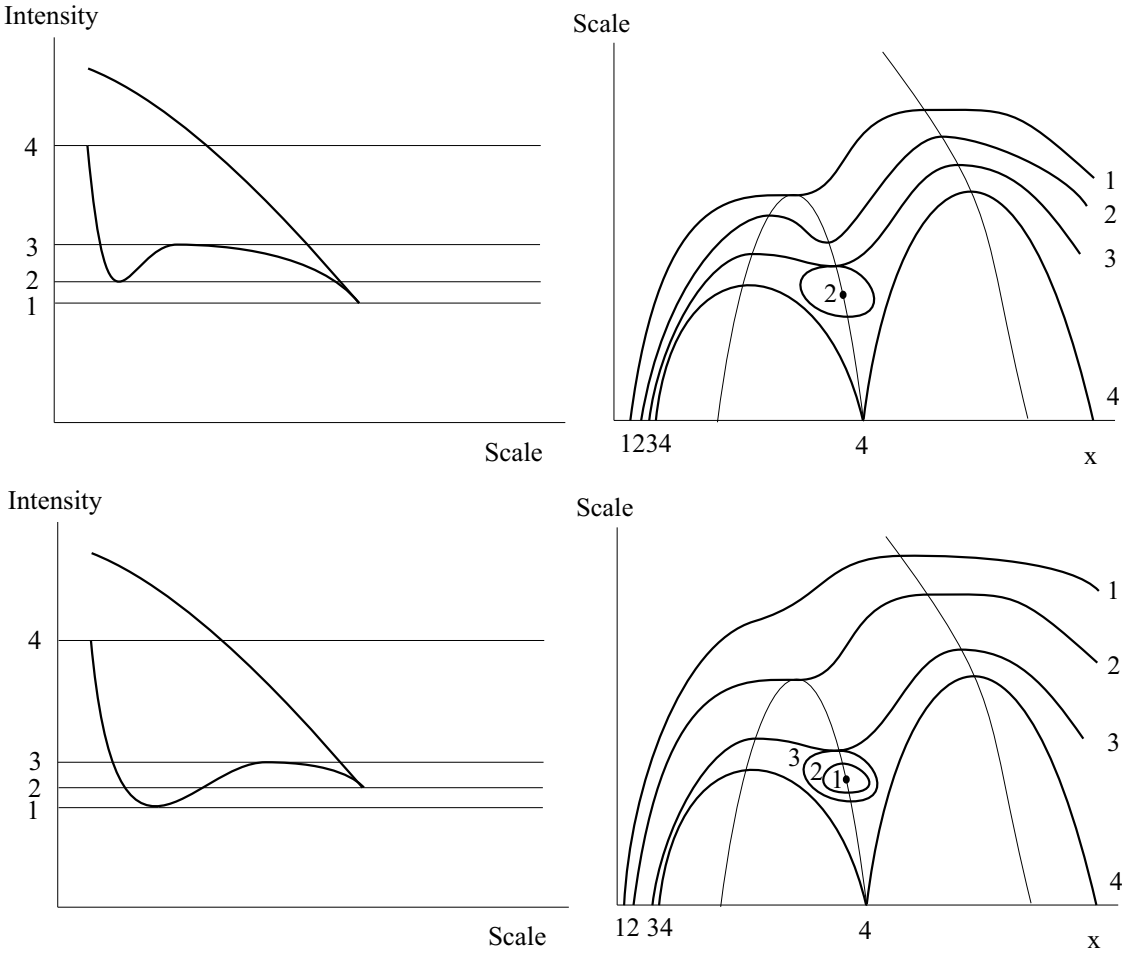

Figure 5: a (Case A) and c (Case B): Intensities of the maximum (top) and saddle branch. b (Case A) and d (Case B): Critical curves (thin) and Iso-intensity manifolds (thick) in the plane of the dominant spatial variable and scale. The two manifolds through the saddle at the initial image are distinct. The scale space saddles each form the self-intersecting locations of one single manifold.

1. **If the highest value of the saddle branch is attained at the initial image, the iso-intensity manifold through this saddle contains two distinct parts. If the branch contains scale space saddles, then at these points manifolds intersect themselves and the scale space saddles are void.**

2. **If the highest value is attained at a scale space saddle, the manifold through it contains two distinct parts. If more scale space saddles are present, the manifolds through them are not distinct and the scale space saddles are void.**

4 Geometry

In this section I describe the global structure of iso-manifolds in $\mathcal{GSS}$ and relate it to the scale space saddles, as well as the hierarchical structure. I will focus on 2D images and 3D $\mathcal{GSS}$ images for visualization purposes, but the results hold in arbitrary dimension.

4.1 Manifolds

From the definition of a $\mathcal{GSS}$ image itself it is clear that 'all thing blur away'. As proven by Loog et al. [35], if the image is padded with zeros (it has infinite support), all critical points stay within the original image (the hull), while at some scale only one extremum remains. Theoretically, at infinite scale all intensities have spread out equally over the image with infinite support, i.e. the average intensity converges to zero. The importance of this result is that there is a scale at which there is only one extremum left in the blurred image.

At this scale in the blurred image, the isophotes form closed curves that can be traced downwards, while the single point forming the extremum forms the top of a dome-shape. What is within this dome cannot be reached given this blurred image [22].

Alternatively, given an arbitrary iso-manifold in the $\mathcal{GSS}$ image, if it intersects an extremum it must intersect it at the top of a local dome (the maximal scale at which the manifold locally exists). Obviously, the manifold can have multiple local tops, although they are located at different scales - just like an arbitrary 1D function generically has extrema with different values. Furthermore, in the $\mathcal{GSS}$ image there is exactly one global top: at that scale the manifold is reduced to an extremum and when scale is increased the manifold disappears.

Consequently, in the $\mathcal{GSS}$ image all iso-manifolds are only open at the original image - the isophotes. Alternatively, all isophotes converge at some scale to circles and disappear when increasing scale. Note that this does not have to happen immediately, as pointed out by Lifshitz and Pizer [33]. They reported the change in curves from non-intersecting to intersecting. This is due to the global structure of iso-manifolds in the neighbourhood of scale space saddles, as will be shown in the next section.

Finally - but perhaps most important, it should be noted that the causality principle states the there are no new level lines - isophotes created when increasing scale. This implies that in the $\mathcal{GSS}$ image it is impossible that an iso-manifold is completely closed (i.e. closed from below). It must have an open end towards the original image. As a result, each isophote at some scale is present in the original image and the critical points in the $\mathcal{GSS}$ image are saddle points. So it remains to investigate the global structure of iso-manifolds through these points.

4.2 Saddles

At spatial saddle points, generically two parts of a manifold are joined or split [13]. For example, one can think of a pair of trousers (join) or the two humps of a camel (split). More special are the scale space saddle, at which two parts have one contact in one point - at least locally [26].

However, only local information of the scale space saddle environment is insufficient. The two parts having contact may be indeed two iso-manifolds that do not share any other common point(s), but they may as well be one and the same manifold. If the latter case applied, the saddle is called 'void' according to [26]. This paper gives a closed definition to distinguish between the two cases, essential to build the hierarchy.

4.3 Contact at saddles

The first item to be addressed is the contact at a scale space saddle. It is commonly said that two manifolds are touching, but this might give the wrong impression. Since the scale space saddle is also a spatial saddle, the isophote in the blurred image through the (scale space) saddle is self-intersecting. This intersection is transversal - there is a non-zero angle between the crossing parts. The two parts bounded by the isophote have a peak and are not isomorphic to a circle. So instead of two spheres touching at the scale space saddle, there are two peaks joined at a single point, see Figure 2a. The manifolds with a small difference in intensity divide in two cases. The first case yields (locally) two manifolds that do not (locally) intersect. The second case consists of one manifold that is tunnel-shaped around the scale space saddle.

4.4 Global structure at saddles

The second item to take into account is the types of critical curves involved. When two distinct manifolds are considered, there are two critical curves that intersect the manifolds at their tops. These critical curves can be either of the same type (both containing either minima or maxima), or of different type (one containing a minimum and one containing a maximum). Visualization of both types can be made easier when regarding the blurred image and the isophote through the (scale space) saddle.

4.4.1 Type 1: same types of critical points

If both curves have the same type, the (scale space) saddle is placed 'in between' both extrema: a 'common' eight-figure appears. In the $\mathcal{GSS}$ image the two iso-intensity manifolds are two juxtaposed peaky kissing domes, the result of two locally dome-like shapes approaching each other, see Figure 6a.

4.4.2 Type 1: different types of critical points

In case of an scale space saddle joining a maximum and a minimum curve, on extremum, say the minimum, is placed in between the saddle and the other extremum (thus being the maximum). This relates to a wrapped eight-figure, where one part lies inside the other. In the $\mathcal{GSS}$ image the minimum-related part of the manifold kisses the outside part of the maximum-related part of the manifold, see Figure 6b.

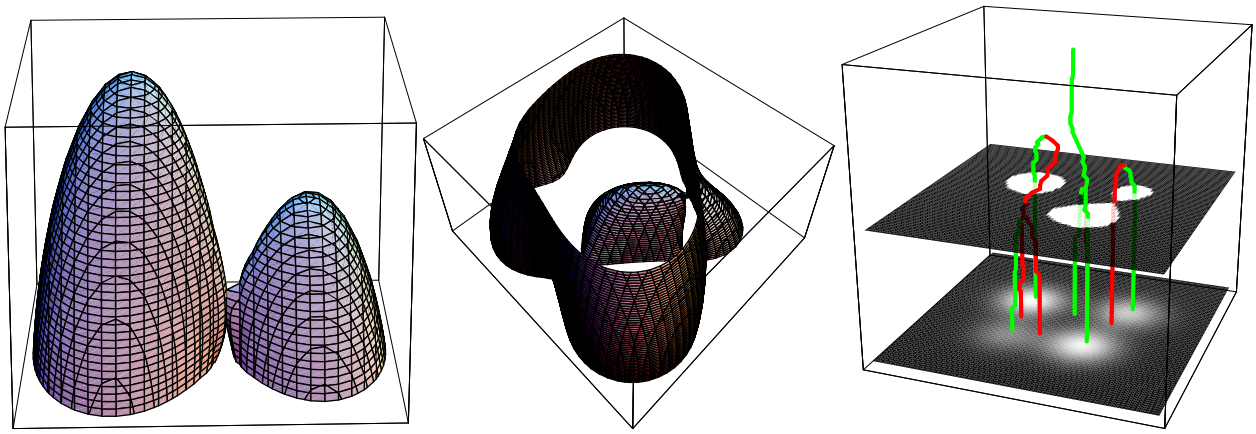

Figure 6: a) Extrema are of the same type: two juxtaposed domes. b) Extrema are of different types: one dome inside the other. c) What will be the geometry of the dual and critical manifolds?.

5 Avoiding 3D Region Growing

Once having obtained the critical curves, the scale space saddles and their relations, there are two major time–consuming things to do (see also Figure 6c).

Firstly, it needs to be determined how the manifolds are shaped at the original image. This is non-trivial, since the manifold may be 'trousers-like', giving rise to (at least) two distinct isophotes in the original image. So a global investigation is needed to find the correct form of the dual manifold. This is depicted in Figure 7. The left images show an intersection of the $\mathcal{GSS}$ image in the (x, t) plane, with x such that the two scale space saddles (the dots) are in the intersection plane. The continuous curves show the dual and critical manifolds (with D and C labels), the dashed curves represents the critical curves (with extremum e and saddle s branches), and the horizontal dashed line is the image at a scale with a scale space saddle (on s_2). The resulting tree structures are shown on the right. Both scaled images contain regions around the extrema e_1, e_2, and e_3. The latter is part of the critical manifold, but for the dual manifold one can see that the top row image has only e_2 as dual part, while the bottom row image has also the e_1 as part of the dual manifold.

Secondly, it needs to be determined what the top of the dual manifold is, or, in another way, to which other critical curve the saddle is related. This is essential for the linking in the tree. In [29] the authors propose a 3D-region growing with the scale space saddle as seed point. This clearly solves the problem, but the shape of manifolds may make this a very time-consuming method. A different method to overcome these problems is proposed.

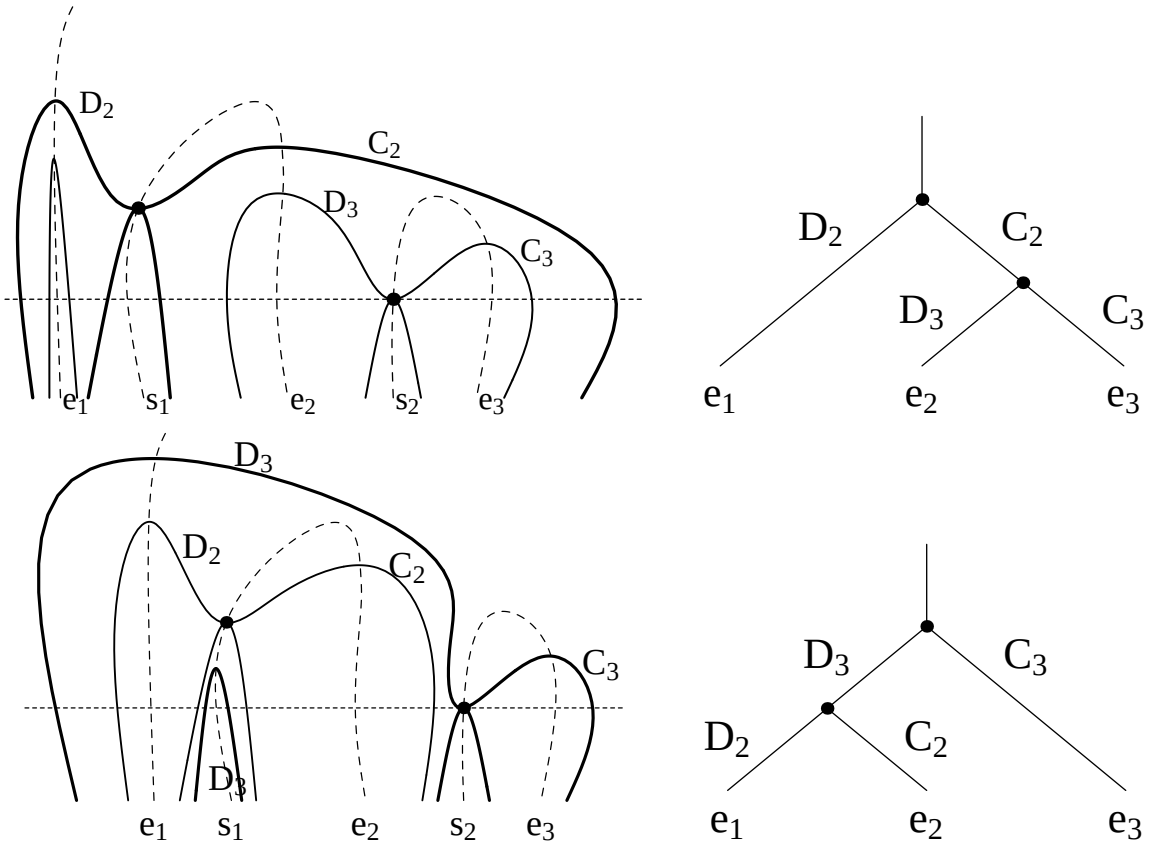

Figure 7: Two scenarios with the same image thresholded at the intensity of the scale space saddle . See text for details.

5.1 Top-finding

To find the top of the dual manifold, it suffices in most cases to find the extrema in the blurred image that are encapsulated by the isophote through the (scale space) saddle. Since the saddle is connected to one extremum in a critical curve, it is clear which of the two areas contribute to the inner part critical manifold. Taking the other part, one finds at least one extremum. If there are multiple extrema, then their intensities along the critical curve are known. So also the intensity of the scale space saddle is located on at least some of these curves. Then it suffices to take the extremum with that intensity that has the highest scale value, i.e. the one located highest in scale. This is the top of the dual dome and the extremum belongs to the critical curve related to that related to the critical manifold. This is the case in Figure 7, top row. The isophote contains the extrema e_3 and e_2. Since the first one vanishes with branch s_2 (containing the scale space saddle), it is part of the critical manifold. The latter extremum has an intensity equal to that of the scale space saddle, where it intersects the dual manifold.

It may happen that the curve doesn't contain the intensity. Then it is involved in a second scale space saddle elsewhere. Then the same procedure is taken for this extremum and the curves link to the dual manifold determined by the last scale space saddle This is the case in Figure 7, bottom row. The isophote contains (again) the extrema e_3 and e_2. Since the first one vanishes with branch s_2 (containing the scale space saddle), it is part of the critical manifold. The latter extremum doesn't have an intensity equal to that of the scale space saddle, but vanishes before it can intersect the manifold determined by the intensity of the scale space saddle. It therefore is a critical manifold, linked by its scale space saddle to extremum branch e_1, being the dual part. Therefore also e_3 is to be linked to this branch. Branch e_1 intersects both manifolds given bye_2 and e_3. The ordering follows by the intensities of these manifolds.

This is sufficient to derive the tree structure, since critical curves can only escape manifolds through their

tops. To find the segments (bounded by isophotes) in the image related to each critical and dual manifold, one needs to follow the next procedure.

5.2 Region shrinking / subtree selections

Given the root of the tree (the remaining extremum in the $\mathcal{GSS}$ image), one also has its intensity. Since this forms the top of some dome in the $\mathcal{GSS}$ image that has an open end at the original image, one can just trace from the boundary of the original image padded with zeros (containing being thus the 'isophote' with value zero) inwardly until the desired intensity is reached. Note that this cannot cause the isophote to be spilt, since all extrema but the remaining one are located within this region[1].

While going down in scale, one finds at one moment the first node, the scale space saddle at which a critical manifold was connected to the remaining extremum. This relates to shrinking the isophote in the original image to the first isophote(s) with the intensity of the scale space saddle. This time, splitting of isophotes in the dual part is possible due to the 'trousers' event. In the critical manifold part, there is exactly one isophote. Obviously, inside the isophote another isophote with the same intensity may occur due to the presence of other extrema.

The simple procedure is justified by the causality principle, regarded downwardly in scale: no level lines (isophotes) disappear.

From the tree point of view, this is just selecting the left subtree at a node being the dual manifold, and the right subtree as the critical manifold. Returning to Figure 7 again, the top row tree simply gives for e_2 the region around e_1 as dual and the regions around e_2 and e_3 as critical, since the top node defines the left and right subtrees. For e_3 it is just e_2 as dual and e_3 as critical. The bottom row tree gives a different result. Now for e_2, e_1 is the dual part and e_2 the critical part, while for e_3 the dual part is obtained by e_1 and e_2.

6 Examples and Applications

In this section I elaborate on the presented method based on two images. Firstly, a blob image is obtained by adding up four Gaussian blobs with different intensities, see Figure 8a. In this way numerical calculations can be verified analytically. Next, an MR image from "BrainWeb[2]" is taken [1, 2, 32], see Figure 16a. These images were also used in [29], providing the dual and critical manifolds obtained by the 3D region growing method. The results of the segmentation and the corresponding speed issues can therefore be compared.

[1] I consider generic images, so binary images are excluded. All non-generic images can be made generic by adding infinitesimal perturbations.

[2] `http://www.bic.mni.mcgill.ca/brainweb`

6.1 Artificial image

In the 81×81 artificial image shown in Figure 8a, five extrema are present of which 4 maxima and one minimum. Its critical curves in scale space (existing of 113 calculated samples that are logarithmically taken) are visualised in Figure 8b. Clearly, four (dark-grey) saddle branches are visible. One extremum branch remains. The intensities of the saddle branches of the critical curves are plotted in Figure 9a. One can see that the

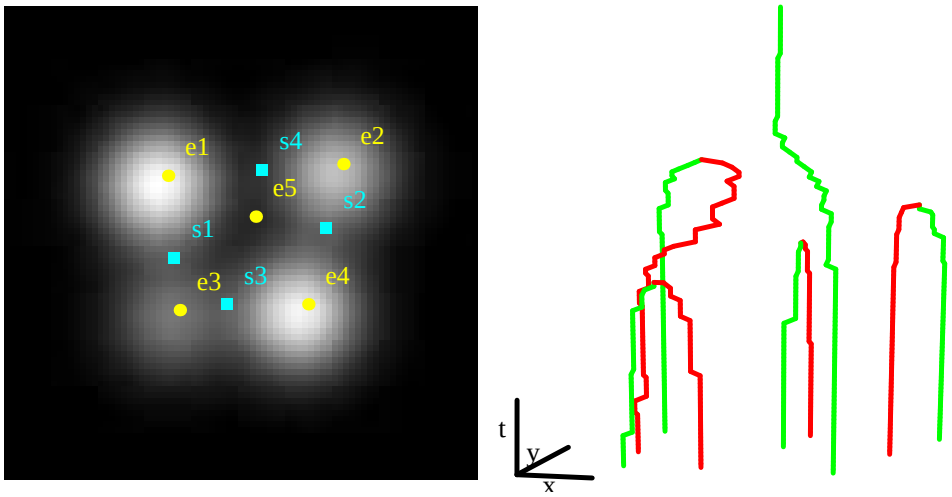

Figure 8: a: Artificial blob image with labels on critical points. b: Its critical curves containing extrema (bright) and saddle (dark) branches.

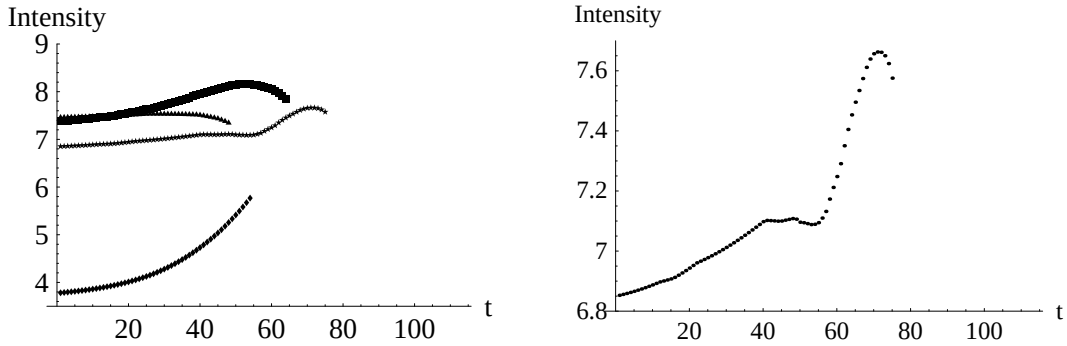

Figure 9: a: Intensities of the saddle branches. b: The saddle branch with multiple scale space saddles around intensity 7.1.

saddle branch with the lowest intensities is monotonically increasing. It annihilates with the minimum, so for segmentation the lowest value on the saddle branch, i.e. the one of the saddle at the initial image, should be taken. The two upper branches both contain one scale space saddle. Of the last saddle branch a close-up is shown in Figure 8b. Around the value of approximately 7.1 four scale space saddles can be seen in the scale sample range 40 to 60. Obviously they are void, and the scale space saddle with maximal intensity is located at approximately 7.66, at scale sample 71.

6.1.1 Zero scale space saddles

The minimum-saddle branch doesn't contain scale space saddles. The iso-intensity manifold in scale space of the value of the saddle at the initial image is shown in Figure 10a. Here two distinct manifolds intersecting each other at the saddle are visible. In contrast, the iso-intensity manifold with the value of the saddle at the catastrophe, Figure 10b, shows only one manifold.

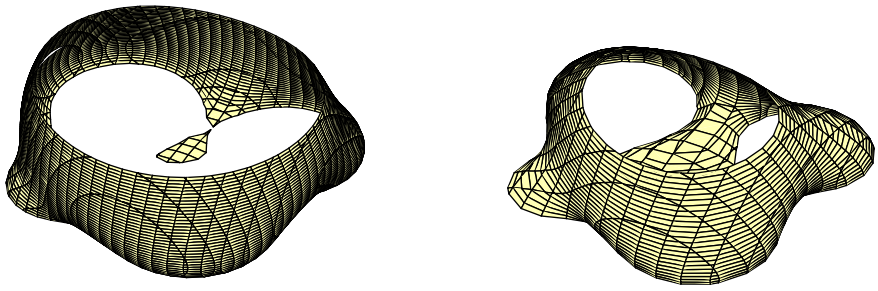

Figure 10: a: Correct iso-intensity manifold for the minimum-saddle pair. b: The wrong one.

6.1.2 Multiple scale space saddles

The iso-intensity manifolds through the correct scale space saddle, in the case of multiple scale space saddles on the saddle branch, is shown in Figure 11. Again, two distinct manifolds (one top-left and one at the right) intersecting each other are clearly visible. A third manifold is isolated and not related to the scale space saddle. Note that the iso-intensity manifolds for the two branches with one scale space saddle on the saddle branch are alike.

If one of the void saddles is chosen, the iso-intensity manifold indeed exists of one single manifold that intersects itself leaving room for a hole, as shown in Figure 11b.

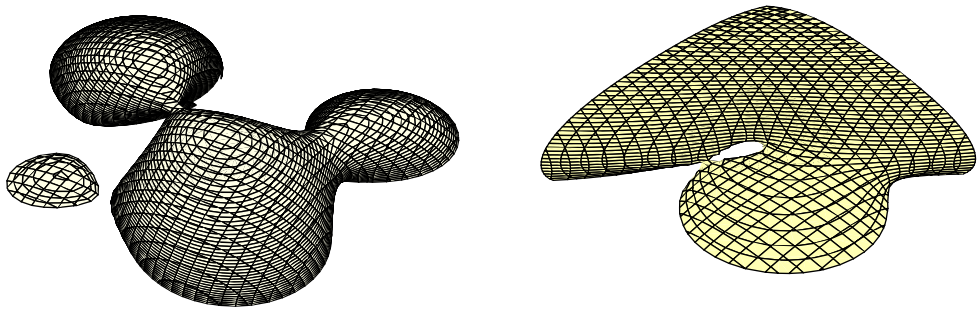

Figure 11: a: Correct iso-intensity manifold for the maximum-saddle pair with multiple scale space saddles. b: Close-up around a iso-intensity manifold through a void scale space saddle.

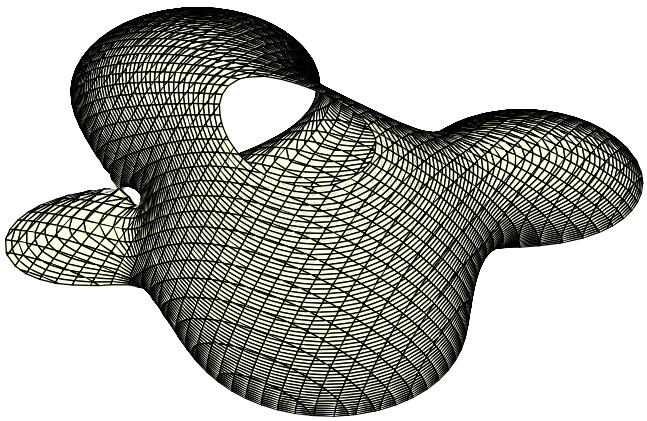

Figure 12: False iso-intensity manifold for the maximum-saddle pair with multiple scale space saddles. The intensity belonging to a void scale space saddle is chosen.

The global situation is visible in Figure 12. It appears that the manifold also encapsulates the extremum bottom-left, in contrast with the correct iso-intensity. As one can see from these images, the extremum top-left in the original image, Figure 8a, is related by the scale space saddle to the two extrema on the right. However, due to the blurring process the extremum bottom-left exhibits a disturbing influence. One may also think of

the saddle being attracted firstly by the extremum bottom-left, but taking a final annihilation relation with the extremum top-left[3]. This is also visible in the behaviour of the critical curves, Figure 8b, where this saddle branch takes a kind of detour before annihilation in contrast to the other saddle branches.

6.1.3 speeding up

For the blob image the critical curves and the image thresholded at the intensity of the scale space saddles are shown in Figure 13. To verify the final results, Figure 14 shows the manifolds through the scales space saddles.

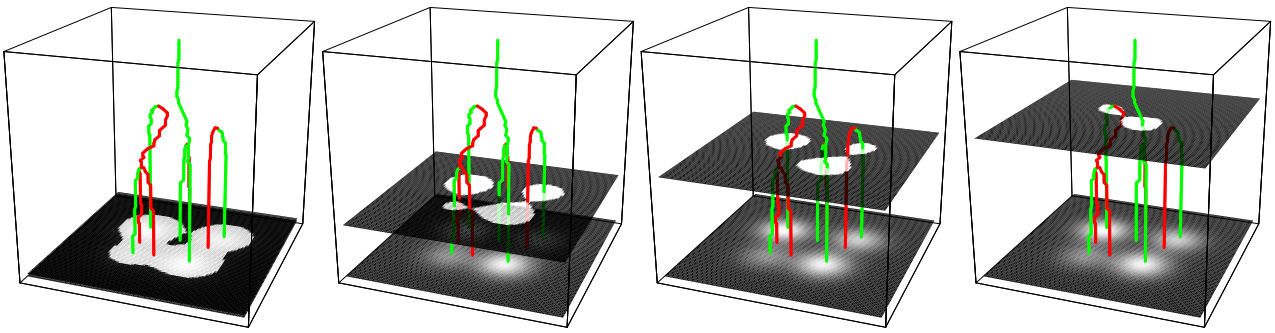

Figure 13: Successive scale space saddles as scale increases with the intensity threshold at the intensity of the scale space saddle. a) e_1 b) e_2 c) e_3 d) e_5

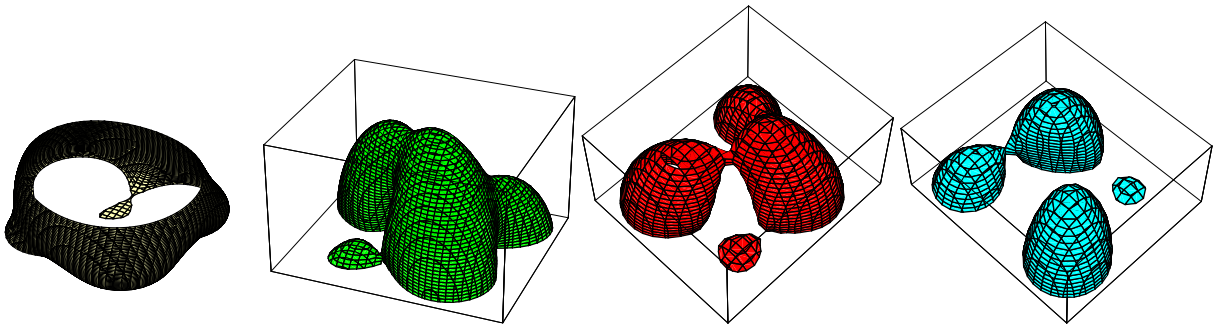

Figure 14: Manifolds in $\mathcal{GSS}$ with the intensities of the scale space saddles, sorted on the intensities of the scale space saddles. a) e_1 b) e_2 c) e_5 d) e_3

Comparing both figures, it is clear that the image at the scale of the scale space saddle (Figure 13) doesn't contain sufficient information. For extremum e_2 the extrema $e_3, e_4,$ and e_5 are in the dual part (b), while for extremum e_3 only e_4 is in the dual part (c) - while there is a part of e_5 visible. For e_5 both e_3 and e_4 are in the dual part (d) - and e_3 isn't even present anymore at this scale. This is not obvious at all from Figure 13, but it is clear given the complete manifolds (Figure 14) .

However, the top-finding procedure returns e_4 as critical curve intersecting the dual manifold at the top in all cases. Next, when building the tree, the scale space saddles are ordered in their intensities. Tracing downwardly from the root, firstly the extremum e_1 is found generating a critical manifold. Note that this is a situation of different types of extrema (Figure 6b). Secondly, e_2 is split off, next e_5, and finally e_3.

The region shrinking procedure then finds the sequence shown in Figure 15. Here black regions denote the parts belonging to the critical manifold, while white regions denote the parts belonging to the dual manifold. Firstly the minimum e_1 is found (top left): a black region within the white (the wrapped eight figure). Secondly, within the white regions the shrinking takes place and e_2 is found as critical (top right), while the parts around the other maxima are part of the dual manifold. These two images still relate to the top rows of the Figures 13 and 14.

[3]One may also imagine the saddle as being rejected by the extremum bottom-left, since it preferred another saddle to annihilate with.

Table 1: Running times of the 2D and 3D region grow based algorithms for the blob image in seconds.

	blobs			
extremum	1	2	3	5
2D	0.470	0.311	0.280	0.291
3D	54.178	61.729	37.614	54.999

The next one that is found is extremum e_5 (bottom left) with e_3 and e_4 as part of the duals. Although this is clear from Figure 14 bottom left, it contradicts the intuition suggested by Figure 13 bottom right. This again warns that scale space is not trivial at all.

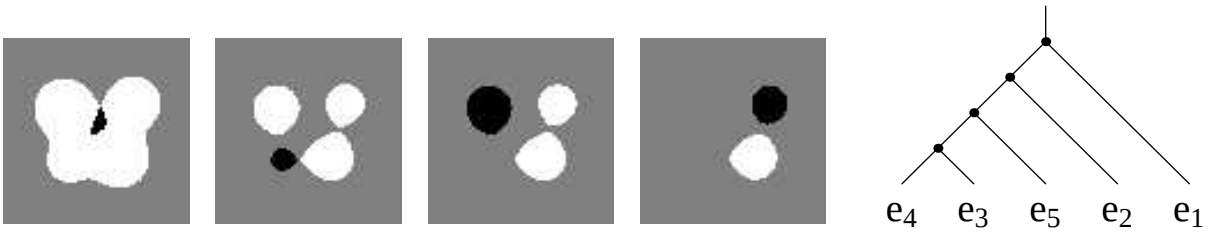

Figure 15: Regions and trees for the blob image found by the shrinking / subtree search method. Black: critical, White: Dual.

Note that these results are identical to the "ground truth" as given in [29].

The main computational gain is given in Table 1. Although the running times are given for non-optimized code, the differences are clear.

6.2 MR image

Secondly the 217×181 MR image of Figure 16a is taken. Since it contains many critical points, the scale space image starting at scale 8.37 is used. This scale is chosen for visualisation purposes, since it yields a reasonable number of critical points to handle with. The first image is visualised in Figure 16b, together with its seven extrema and six saddle points. A scale space containing 87 scales was built and critical paths were calculated.

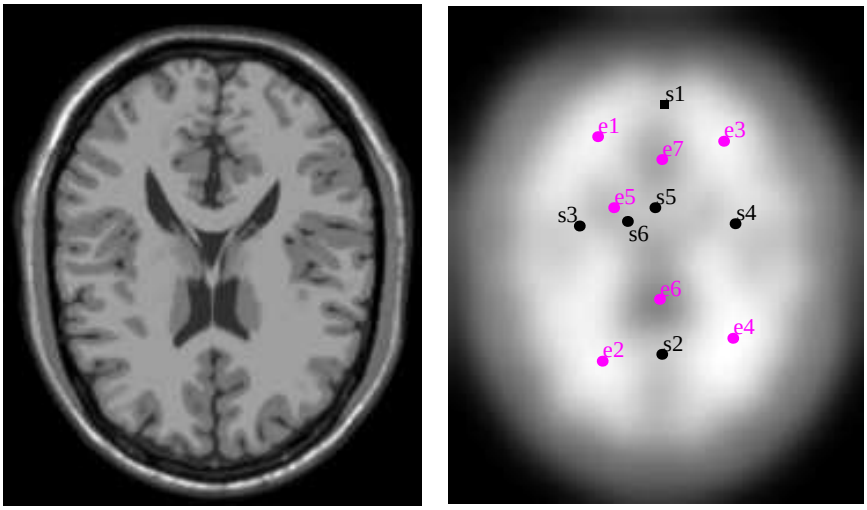

Figure 16: a) MR image. b) Image on scale 8.37, with the labelled spatial critical points: seven extrema and six saddles.

6.2.1 Scale space saddles

The intensities of some of them are shown in Figure 17.

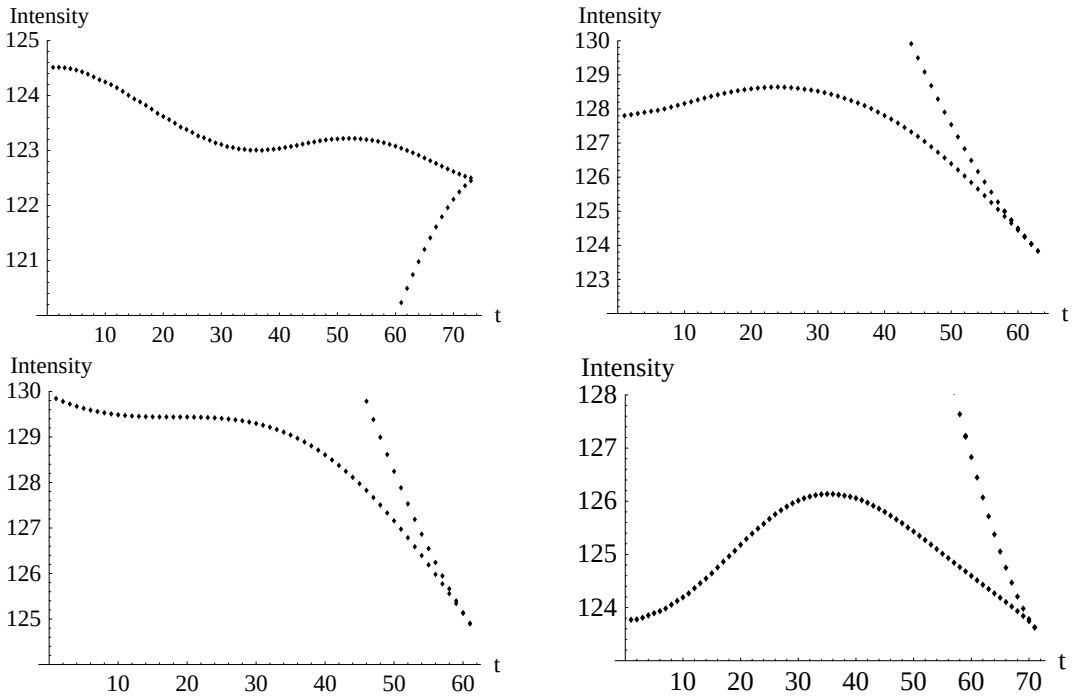

Figure 17: Intensities of the critical curves combing the critical points From left to right, top to bottom: a) e6-s1 b) e1-s3 c) e3-s4 d) e2-s2.

The various types of scale space saddle point occurrences are present in this sequence.

- **Clearly, the first graph shows non-generic behaviour since the annihilation coincides with the scale space saddle. Furthermore two void scale space saddles are present but both not affect the proposed segmentation since they are both larger than the intensity of the annihilation (in this case it is a minimum annihilating).**
- **The second graph shows the "standard" situation when the intensity of the scale space saddle is larger than the annihilation intensity.**
- **The third graph shown a monotonically decreasing saddle intensity and thus corresponds to the zero scale space saddle situation.**
- **The last graph again shows the "standard" situation, although the situation of the saddle branch around the first scales may give rise to the assumption that there also a (void) scale space saddle is located.**

The segments corresponding to the intensities of the correct values of the scale space saddles (and initial saddle for the third curve) are shown in the top row of Figure 18.

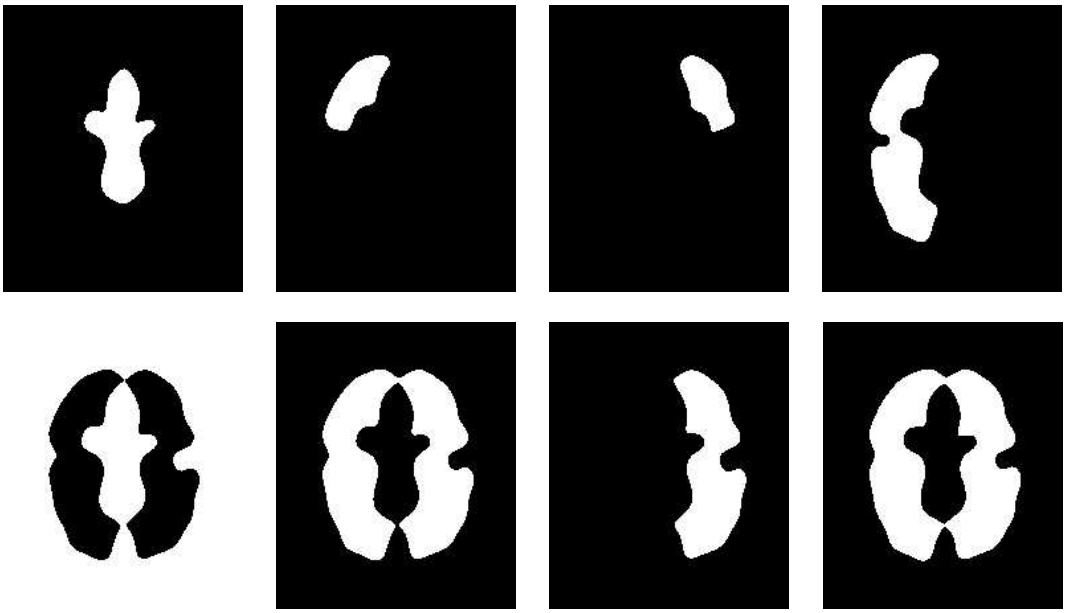

Figure 18: Shown in white are the segments of Figure 16b determined by the critical curves of Figure 17. They correspond to, from left to right, the extrema e6, e1,e3, and e2. The top row depicts the correct selection of the intensity values, while the bottom row gives an example of a selection of wrong values. Note that the segment belonging to e2 *does* encapsulate e1 (top row), but *does not* encapsulate e3, cf. [24, 30, 31].

6.2.2 Void scale space saddles

To show that one should be careful, in the bottom row the segments corresponding to false intensity values are shown: The initial saddle for the minimum (left) and annihilation intensities for the three maxima (second to forth). For the minimum inside the brain, background is selected for this false intensity. As can be seen in Figure 18, bottom left, the connection from the inner part to the exterior is made via a saddle connecting the parts related to the left and right maxima's, cf. the second and third image in the top row of Figure 18. Just as in the previous section a void saddle is chosen. The consequence for this in the original image is shown in Figure 19. To the left the correct segment is shown, while the white segment of Figure 19b is clearly connected to the background

The regions belonging to the maxima regions become at least twice as large. Here the problematic – and wrong – situation occurs that two regions are found that encapsulate the same number of extrema, viz. the second and the last image of the bottom row of Figure 18. This obviously violates the uniqueness of the hierarchy.

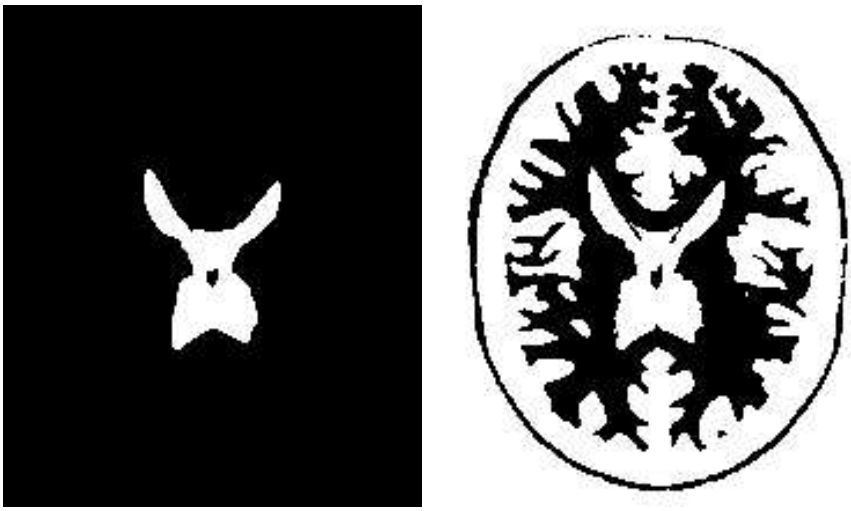

Figure 19: Segment of extremum e6 of Figure 16a – the unblurred MR image – according to the a) correct, and b) wrong intensity value, cf. Figure 18 top left and bottom left, respectively.

6.2.3 speeding up

The region shrinking procedure applied to the MR finds the sequence shown in Figure 20. Here black regions denote the parts belonging to the critical manifold, while white regions denote the parts belonging to the dual manifold. These results are identical to the "ground truth" as given in [29]. Here the images are derived from the subtree search. For example, the first image obtained $C(e_6)$ as the union of regions around e_5, e_6, and e_7, and $D(e_6)$ as the union of regions around e_1, e_2, e_3, and e_4, since the scale space saddle related to e_6 is the top node in the tree (see also [29]). This scale space saddle is of type 2, combining different types of critical points.

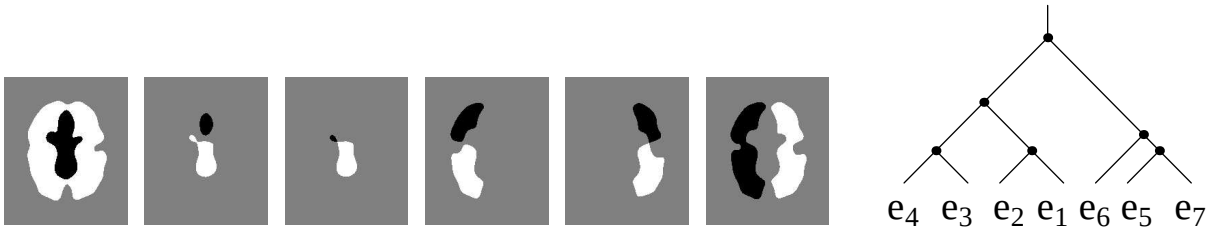

Figure 20: Regions and trees for the MR image found by the shrinking / subtree search method. Black: critical, White: Dual.

The main computational gain is given in Table 2. Although the running times are given for non-optimized code, the differences are clear.

Table 2: Running times of the 2D and 3D region grow based algorithms for the MR image in seconds.

	MRI					
extremum	1	2	3	5	6	7
2D	1.021	0.601	0.551	0.721	0.371	0.721
3D	2360.1	649.183	731.281	354.98	238.694	522.01

7 Conclusion and Discussion

In this paper I investigated and discussed the geometry of iso-intensity manifolds through scale space saddles in scale space. They can be classified into two essentially different cases. The first set consists of manifolds that have only one point in common, the scale space saddle. Each manifold yields a pair of manifolds with the same intensity if the scale space saddle is removed. The second set is formed by the manifolds that self-intersect. If the scale space saddle is removed from such a manifold, still one manifold remains. The scale space saddle in case is defined as *void*.

For the scale space hierarchy (tree) and segmentation it is essential that scale space saddles yielding manifolds from the first set are taken. Then for each extremum in the initial image a unique region can be assigned, together with the region to which it hierarchically belongs. In some cases - if the number of scale space saddles on the saddle branch is even - the spatial saddle at the initial scale must also be taken into account.

Since each scale space saddle is related to an extremum by means of the critical curve, to each extremum a unique (scale space) saddle is assigned. A procedure to select the correct (scale space) saddle is given: considering a maximum-saddle pair, the saddle with the highest intensity is to be assigned to the maximum. For a minimum the opposite holds.

More details of the algorithm to derive the hierarchy tree, the use of it and several applications, can be found elsewhere [24, 30, 31]. In case of multiple scale space saddles on a saddle branch of the critical curve, the procedure as described above was used, albeit without justification.

Next, the local behaviour at the scale space saddles was clarified, distinguishing two essentially different kinds of interactions of manifolds at scale space saddles. Furthermore it was shown what the global structure of manifolds in $\mathcal{GSS}$ images looks like and how it can be used.

This links the known local events in Gaussian scale space with the global hierarchy and segmentation method proposed in [26, 29]. This method relies on an $(n+1)-$dimensional region growing procedure to find relevant structures (i.e. the geometry of certain manifolds) and can be heavily time consuming.

Using the presented investigation of the geometry of $\mathcal{GSS}$ images, a region growing algorithm in the full $\mathcal{GSS}$ image in order to find the tree structure, can be avoided. It suffices to do a region growing on the scaled image only, in combination with a linear search along critical curves to find the hierarchy tree. Furthermore, a locally $(n-1)-$dimensional manifold shrinking in the original image, or (equivalently) a subtree search and region expanding around the found leaves, suffices to derive the segmentation of the image.

Examples show the appearance of the various described manifolds and relevance of the selection procedure, as well as the much faster running times to derive the tree structures and segmentations.

Therefore the algorithms get a significantly less complexity, enabling faster use in image recognition and comparison as presented in e.g. [20].

Acknowledgements

This work was supported by the IST Programme of the European Union (IST-2001-35443) and Senter-IOP grant IBV99006. The author would like to thank Luc Florack of Eindhoven University of Technology, the Netherlands, for stimulating discussions leading to this research.

References

[1] C. A. Cocosco, V. Kollokian, R. K.-S. Kwan, and A. C. Evans. Brainweb: Online interface to a 3D MRI simulated brain database. In *NeuroImage, vol.5, no.4, part 2/4, S425, 1997 – Proceedings of 3-rd International Conference on Functional Mapping of the Human Brain, Copenhagen, May*, 1997.

[2] D. L. Collins, A. P. Zijdenbos, V. Kollokian, J. G. Sled, N. J. Kabani, C. J. Holmes, and A. C. Evans. Design and construction of a realistic digital brain phantom. *IEEE Transactions on Medical Imaging*, 17(3):463–468, 1998.

[3] J. Damon. Local Morse theory for solutions to the heat equation and Gaussian blurring. *Journal of Differential Equations*, 115(2):386–401, 1995.

[4] J. Damon. Local Morse theory for Gaussian blurred functions. In *Sporring et al. [39]*, pages 147–162, 1997.

[5] R. Duits, L. M. J. Florack, J. de Graaf, and B. M. ter Haar Romeny. On the axioms of scale space theory. *Journal of Mathematical Imaging and Vision*, 20(3):267–298, 2004.

[6] D. Eberly. A differential geometric approach to anisotropic diffusion. In *ter Haar Romeny, [15]*, pages 371–392, 1994.

[7] M. Fidrich. Iso-surface extraction in 4-D with applications related to scale space. In *Proceedings of DGCI'96, 6th International Conference on Discrete Geometry for Computer Imagery (Lyon, France, November 1996)*, pages 257–268, 1996. Lecture Notes in Computer Science 1176.

[8] M. Fidrich. Following feature lines across scale. In *ter Haar Romeny et al. [17]*, pages 140–151, 1997.

[9] M. Fidrich. Iso-surface extraction in n-D applied to tracking feature curves across scale. *Image and Vision Computing*, 16(8):545–556, 1998.

[10] L. M. J. Florack. *Image Structure*, volume 10 of *Computational Imaging and Vision Series*. Kluwer Academic Publishers, Dordrecht, The Netherlands, 1997.

[11] L. M. J. Florack and A. Kuijper. The topological structure of scale-space images. *Journal of Mathematical Imaging and Vision*, 12(1):65–80, February 2000.

[12] L. M. J. Florack, B. M. ter Haar Romeny, J. J. Koenderink, and M. A. Viergever. Linear scale-space. *Journal of Mathematical Imaging and Vision*, 4(4):325–351, 1994.

[13] L. D. Griffi n and A. Colchester. Superfi cial and deep structure in linear diffusion scale space: Isophotes, critical points and separatrices. *Image and Vision Computing*, 13(7):543–557, September 1995.

[14] L.D. Griffi n and M. Lillholm, editors. *Scale Space Methods in Computer Vision*, volume 2695 of *Lecture Notes in Computer Science*. Springer -Verlag, Berlin Heidelberg, 2003.

[15] B. M. ter Haar Romeny, editor. *Geometry-Driven Diffusion in Computer Vision*, volume 1 of *Computational Imaging and Vision Series*. Kluwer Academic Publishers, Dordrecht, 1994.

[16] B. M. ter Haar Romeny. *Front-end vision and multi-scale image analysis*, volume 27 of *Computational Imaging and Vision Series*. Kluwer Academic Publishers, Dordrecht, The Netherlands, 2003.

[17] B. M. ter Haar Romeny, L. M. J. Florack, J. J. Koenderink, and M. A. Viergever, editors. *Scale-Space Theory in Computer Vision: Proceedings of the First International Conference, Scale-Space'97, Utrecht, The Netherlands*, volume 1252 of *Lecture Notes in Computer Science*. Springer-Verlag, Berlin, July 1997.

[18] T. Iijima. Basic theory of pattern normalization (for the case of a typical one dimensional pattern). *Bulletin of the Electrotechnical Laboratory*, 26:368– 388, 1962. (in Japanese).

[19] T. Iijima. On the Gaussian scale-space. *IEICE Japan, Trans. D*, E86-D(7):1162–1164, 2003.

[20] F. Kanters, B. Platel, L. M. J. Florack, and B.M. ter Haar Romeny. Content based image retrieval using multiscale top points. In *Griffin and Lillholm [14]*, pages 33–43, 2003.

[21] M. Kerckhove, editor. *Scale-Space and Morphology in Computer Vision*, volume 2106 of *Lecture Notes in Computer Science*. Springer -Verlag, Berlin Heidelberg, 2001.

[22] J. J. Koenderink. The structure of images. *Biological Cybernetics*, 50:363–370, 1984.

[23] J. J. Koenderink. A hitherto unnoticed singularity of scale-space. *IEEE Transactions on Pattern Analysis and Machine Intelligence*, 11(11):1222–1224, 1989.

[24] A. Kuijper. *The Deep Structure of Gaussian Scale Space Images*. PhD thesis, Utrecht University, 2002.

[25] A. Kuijper. On manifolds in Gaussian scale space. In *Griffin and Lillholm [14]*, pages 1–16, 2003.

[26] A. Kuijper and L. M. J. Florack. Hierarchical pre-segmentation without prior knowledge. In *Proceedings of the 8th International Conference on Computer Vision (Vancouver, Canada, July 9–12, 2001)*, pages 487–493, 2001.

[27] **A. Kuijper and L. M. J. Florack. The relevance of non-generic events in scale space. In *Proceedings of the 7th European Conference on Computer Vision (Copenhagen, Denmark, May 28–31, 2002)*, pages 190–204, 2002.**

[28] **A. Kuijper and L. M. J. Florack. Understanding and modeling the evolution of critical points under Gaussian blurring. In *Proceedings of the 7th European Conference on Computer Vision (Copenhagen, Denmark, May 28–31, 2002)*, pages 143–157, 2002.**

[29] **A. Kuijper and L. M. J. Florack. The hierarchical structure of images. *IEEE Transactions on Image Processing*, 12(9):1067–1079, 2003.**

[30] **A. Kuijper and L. M. J. Florack. Using catastrophe theory to derive trees from images. *Journal of Mathematical Imaging and Vision*, ..(..):..–.., 2004. accepted for publication.**

[31] **A. Kuijper, L. M. J. Florack, and M. A. Viergever. Scale space hierarchy. *Journal of Mathematical Imaging and Vision*, 18(2):169–189, April 2003.**

[32] **R. K.-S. Kwan, A. C. Evans, and G. B. Pike. An extensible MRI simulator for post-processing evaluation. In *Visualization in Biomedical Computing (VBC'96). Lecture Notes in Computer Science, vol. 1131. Springer-Verlag, pages 135-140*, 1996.**

[33] **L. M. Lifshitz and S. M. Pizer. A multiresolution hierarchical approach to image segmentation based on intensity extrema. *IEEE Transactions on Pattern Analysis and Machine Intelligence*, 12(6):529–540, 1990.**

[34] **T. Lindeberg. *Scale-Space Theory in Computer Vision*. The Kluwer International Series in Engineering and Computer Science. Kluwer Academic Publishers, 1994.**

[35] **M. Loog, J. J. Duistermaat, and L. M. J. Florack. On the behavior of spatial critical points under Gaussian blurring, a folklore theorem and scale-space constraints. In *Kerckhove [21]*, pages 183–192, 2001.**

[36] **M. Nielsen, P. Johansen, O. Fogh Olsen, and J. Weickert, editors. *Scale-Space Theories in Computer Vision*, volume 1682 of *Lecture Notes in Computer Science*. Springer -Verlag, Berlin Heidelberg, 1999.**

[37] **T. Poston and I. N. Stewart. *Catastrophe Theory and its Applications*. Pitman, London, 1978.**

[38] **L. Schwartz. *Théorie des Distributions*, volume I, II of *Actualités scientifiques et industrielles; 1091,1122*. Publications de l'Institut de Mathématique de l'Université de Strasbourg, Paris, 1950–1951.**

[39] **J. Sporring, M. Nielsen, L. M. J. Florack, and P. Johansen, editors. *Gaussian Scale-Space Theory*, volume 8 of *Computational Imaging and Vision Series*. Kluwer Academic Publishers, Dordrecht, second edition, 1997.**

[40] **J. A. Weickert. *Anisotropic Diffusion in Image Processing*. Teubner, Stuttgart, 1998.**

[41] **A. P. Witkin. Scale-space filtering. In *Proceedings of the Eighth International Joint Conference on Artificial Intelligence*, pages 1019–1022, 1983.**